Free-space microwave focusing by a negative-index gradient lens

T. Driscoll[a)] and D. N. Basov
University of California San Diego, Physics Department, 9500 Gilman Drive, La Jolla, California 92093

A. F. Starr
SensorMetrix, Incorporated, 5965 Pacific Center Boulevard, Suite 701, San Diego, California 92121

P. M. Rye and S. Nemat-Nasser
University of California, San Diego, CEAM group, MAE Department, 9500 Gilman Drive, La Jolla, California 92093-0416

D. Schurig and D. R. Smith
Duke University, ECE Department, Box 90291, Durham, North Carolina 27708

Metamaterial structures designed to have simultaneously negative permittivity and permeability are known as left-handed materials. Their complexity and our understanding of their properties have advanced rapidly to the point where direct applications are now viable. We present a radial gradient-index lens with an index of refraction ranging from −2.67 (edge) to −0.97 (center). Experimentally, we find that the lens can produce field intensities at the focus that are greater than that of the incident plane wave. These results are obtained at 10.3 GHz and in excellent agreement with full-wave simulations. We also demonstrate an advanced fabrication technique using conventional printed circuit board technology which offers significant design, mechanical, and cost advantages over other microwave lens constructions. © *2006 American Institute of Physics*. [DOI: 10.1063/1.2174088]

Since their first realization in 1999 by Smith *et al.*[1]—guided by the earlier theoretical work of Veselago[2]—understanding of negative index materials (NIMs) has advanced rapidly. Metamaterial-style structures with negative index of refraction ($n = \sqrt{\varepsilon}\sqrt{\mu}$) were initially constructed and tested at microwave frequencies.[3,4] They have since advanced through infrared,[5,6] and are now at a stage where direct applications are within reach. To date, these structures have largely been of the "wine-crate" construction,[7] which is an array of split-ring resonators (SRRs) and wires. This construction, while useful in demonstrating the basic phenomenon, lacks structural integrity and is time consuming to construct, and limits design complexity.[8,9] Limitations in design tolerance and material in wine-crate metamaterials have also hindered the progress of experimental positive-gain lensing using NIMs. Given the recent evidence showing the superiority of NIM lenses in many situations,[10] there is much interest in pushing NIM lenses toward applications.

Here, we present a radial GRIN lens, built from elements similar to the SRRs and wires of previous experiments,[7] but integrated into a fabrication technique using traditional printed circuit board (PCB) technology.[11] Our durable, lightweight, and modular lens operates as a positive gain spherical lens, focusing in two dimensions to achieve a focal spot amplitude +7 dB over incident. This represents a significant advance toward applications, as well as steps forward in design complexity and construction technique.

Using ray-tracing software written in MATHMATICA, we designed a biplanar (geometrically "flat") lens with a radially varying gradient given in

$$\varepsilon(r,\omega) = \mu(r,\omega) = n(r,\omega) = -0.97 - 7.30r^2 + 0.18r^4. \quad (1)$$

A 2 mm thick disk, 15 cm in radius, with this gradient is shown to behave as an $f/9$ lens. In transferring this lens design to our metamaterial, the radial gradient is mapped onto a Cartesian array of unit cells with 50 steps over the radius. Each unit cell is a SRR and wire, shaped to have a specific magnetic and electric resonance. The result is a disk of ∼8000 unit cells [see Fig. 1(a)], nearly one-quarter of which are unique. This large number of steps gives an excellent approximation of a continuous gradient.[12]

To meet the required optical parameters at each unit cell, many variations of the geometry shown in Fig. 1(c) were simulated for *S* parameters in the commercial software package HFSS by Ansoft. The geometry variations involved changing the wire thickness and location and the capacitor-gap pad radius. A standard retrieval method[11] was used to obtain real and imaginary electric permittivity $\varepsilon(\omega)$ and magnetic permeability $\mu(\omega)$ from the simulation *S* parameters. Ten geometries were optimized to span the desired index range at an operating frequency of 10.1 GHz. The optimization goals, in addition to correct index, included matched impedance, low loss tangents, and insensitivity to small geometric changes. The effects of wire thickness, wire location, and capacitor area on the electromagnetic parameters are intertwined, making the design a process relying largely on experience and iterative refinement. We can, however, still identify some variables as heavily influential on particular electromagnetic properties. The parametric graph in Fig. 2 illustrates the dependence of the index on the wire spacing and capacitor pad radius. The circular data points are structures which were simulated as described above, and the square data points interpolated points. The impedance ($Z = \sqrt{\varepsilon/\mu}$) throughout is almost constant, at 1.06 ± 0.05. This is achieved by additionally varying the wire thickness, which

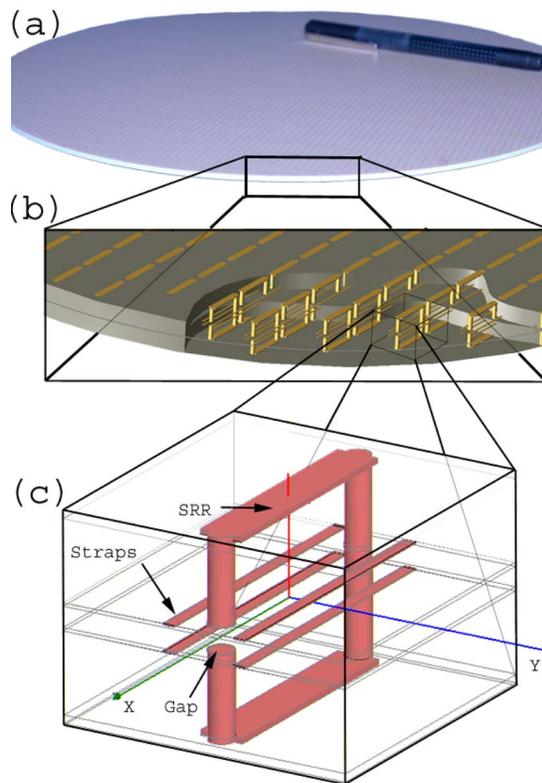a)Electronic mail: tdriscol@physics.ucsd.edu

FIG. 1. Three tier diagram showing (a) actual picture of a lens disk, (b) blow-up illustrating unit-cell array, (c) further blown up single unit cell with SRR and wire elements. Magnetic field is applied in along Y direction, electric field is along X.
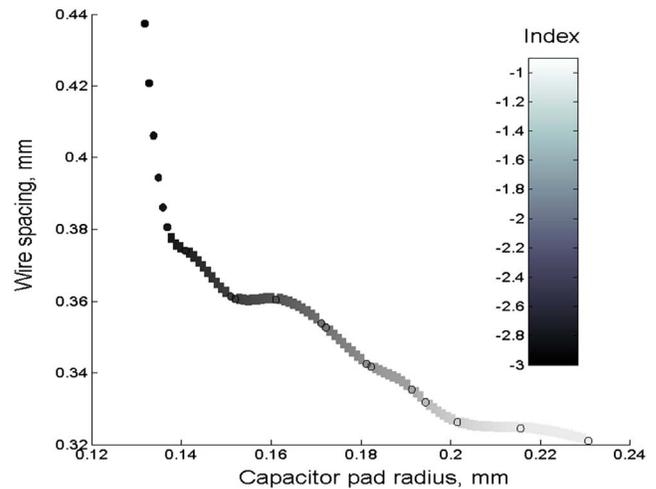

FIG. 2. Parametric plot of index of refraction as a function of wire spacing and capacitor pad radius. The wire thickness (not plotted) is varied to keep the impedance constant ($z=1.06\pm0.05$) throughout. Simulation points shown in outlined circles, squares are interpolated.

predominantly affects the impedance. Each data point in Fig. 2 represents one possible unit-cell design, like the one shown in Fig. 1(c). These unit cells were then arranged in a two-dimensional array in the *X-Y* plane, as shown in Fig. 1(b). This creates a PCB disk 2 mm thick and 30 cm in diameter (pictured in Fig. 1(a)), that responds to a single polarization. These disks can be stacked up to decrease the lens *f/* number approximately linearly, resulting in a highly modular design.

For testing, a microwave compact antenna test range was developed using an off-axis parabolic reflector coupled with a standard feed horn. The polarized plane wave coming off the dish shows moderately good amplitude uniformity—to within ~2 dB over the lens face. The lens is embedded in a styrofoam barrier with $\varepsilon=1.03$, $\mu=1$, and is oriented normal to the plane wave in such a way that the incident electric and magnetic fields lie in the plane of the lens and are aligned to excite the wires and rings, respectively. Our plane wave is measured to have very low cross polarization (<30 dB) which allows us to neglect effects of the structure anisotropy in this experiment. The image side of the lens is scanned in volume using a dipole detector, guided by a *xyz* translation stage as sketched in Fig. 3. The source and detector are connected to a Vector network analyzer, which performs a frequency sweep at each spatial point. Data are collected in a four-dimensional array: In *XYZ* volume over 24 cm by 30 cm by 54 cm, and between 8 GHz and 12 GHz every 0.04 GHz. These data are taken for various thicknesses of lens.

In analyzing these data, we take into consideration that at ~10 GHz, our lens is only ~10λ in diameter—and, the diffractive edge effects may play an important role in its behavior. We wish to consider those lens thicknesses which

will reduce diffractive effects by minimizing the difference in optical path length between two rays passing through and by the edge of the lens:

$$\Delta\phi_{\text{OPL}} = 2\pi d \frac{(n_0 - n_1)}{\lambda_0}. \tag{2}$$

Solving Eq. (2) at the lens edge ($n_1=-2.67$) the first two thicknesses which result in an integer 2π phase difference are $d_1=8.1$ mm and $d_2=16.2$ mm. Each lens disk is 2 mm thick, so a lens constructed of four or eight layers will minimize the influence of diffractive effects in the focal field. Here, we present these two thicknesses; the interesting behavior of highly diffractive small lenses will be considered in a future work.

Shown below in Fig. 3 are data for an eight-layer lens (in black) and a four-layer lens (in gray). Dashed lines are experimental data for the root-mean-square (rms) field amplitude along the optical axis ($x=0$, $y=0$, translate z) at 10.3 GHz, normalized to incident field amplitude. Solid
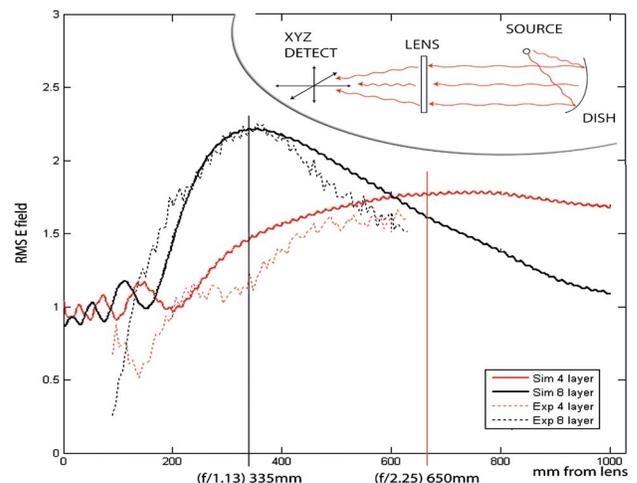

FIG. 3. rms electric-field amplitude in both simulation (solid) and experiment (dash) along the optical axis for GRIN lenses comprised of eight layers (black) and four layers (red).

curves are Microwave Studio simulation results for the same eight- layer and four-layer lenses, the details of which will be discussed presently.

Returning to Fig. 3, we find good agreement between the experimental and simulation results for both the eight- and four-layer lenses. We also find good agreement with the predictions of geometric optics, as determined by our ray-tracing software. Our eight- layer and four-layer lenses have *f*-numbers of 1.13 and 2.25, respectively. The focal lengths predicted by these *f*-numbers are marked as vertical lines in Fig. 3. The eight-layer lens focuses almost exactly where predicted, and though the physical limitation of our scanning stage does not allow enough *z*-axis translation to reach the four-layer predicted focus, the line shape is still in good agreement with simulation.

Microwave Studio simulations are done in the form of a two-dimensional "slice" of the lens along its diameter in order to reduce simulation size. Simulations use 50 unit cells across the lens radius, where each unit cell has been assigned a Lorentzian dispersion in both $\varepsilon(\omega)$ and $\mu(\omega)$, designed such that the index and loss-tangent at 10.1 GHz are very close to the design values. We find only a 2% difference between the design frequency of 10.1 GHz and what we determine to be the best operation frequency at 10.3 GHz. This small shift is likely due to tolerances in both the PCB construction, and the dielectric. Our unit-cell designs call for a tolerance of 1 mil (25 μm), which is at the current limit of technology offered by board fabrication vendors. Fabrication errors, such as registration misalignment, would cause a shift in the parameters of all unit cells. Similarly, an increase in the board dielectric of only 4% would cause a shift in operation frequency near that observed.

The amplitudes in Fig. 3 are with respect to incident rms amplitude 1, with simulation and experiment normalized separately and not relative to each other. As well as showing strong support for the accuracy of our design and fabrication, this illustrates another important feature of this lens: It produces field intensities at the focus that are much greater than that of the incident plane wave. Many researchers have been concerned that losses in existing left-handed materials would preclude their use in real applications. Here, we have demonstrated otherwise. The intentional impedance matching of each unit cell to air, and low loss tangents, result in decreased back reflection and absorption respectively. The peak amplitude of the eight-layer lens focus is nearly 7 dB greater than the incident wave amplitude.

A cross-sectional display of the field amplitude in the *XY* plane at the focal length (Fig. 4 checkered surface) nicely illustrates this gain peak above the average incident amplitude (translucent plane). The solid black line is the beam focus one-dimensional profile from the Microwave Studio simulations, showing fairly good agreement of the expected airy profile.

In conclusion, we have constructed a biplanar gradient lens whose gradient ranges from $n=-0.97$ to $n=-2.67$, and shown the focusing characteristics to be in excellent agreement with simulation. As well as providing experimental confirmation of the behavior of negative-index gradient lenses, the adaptation of conventional PCB fabrication to the wires and SRR elements immensely simplifies the construction of metamaterial lenses. Our gradient lens with nearly
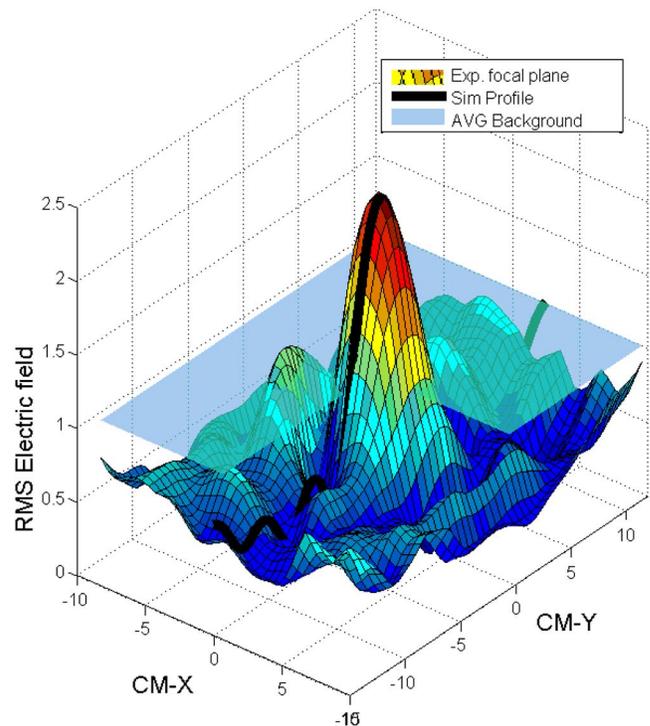

FIG. 4. Two-dimensional profile of the E-field at the eight-layer lens focal plane (solid colored checker). Simulation one-dimensional focus profile overlayed (black line). No-lens averaged background (transparent plane) shown to emphasize magnification.

2000 unique unit cells represents the ultimate test of this recently pioneered construction technique.[8] Experimental demonstration of positive-gain lensing using metamaterials represents an important step towards dealing with the losses often inherent in these materials, highly suitable for aerospace and radar application.

[1] D. R. Smith, W. J. Padilla, D. C. Vier, S. C. Nemat-Nasser, and S. Schultz, Phys. Rev. Lett. **84**, 4184 (2000).
[2] V. G. Veselago, Sov. Phys. Usp. **10**, 509 (1968).
[3] A. A. Houck, J. B. Brock, and I. L. Chuang, Phys. Rev. Lett. **90**, 137401 (2003).
[4] P. Vodo, P. V. Parimi, W. T. Lu, and S. Sridhar, Appl. Phys. Lett. **86**, 201108 (2005).
[5] A.-C. Hsu, Y.-K. Cheng, K.-H. Chen, J.-L. Chern, S.-C. Wu, C.-F. Chen, H. Chang, Y.-H. Lien, and J.-T. Shy, Jpn. J. Appl. Phys., Part 2 **43**, L176 (2004).
[6] S. Linden, C. Enkrich, M. Wegener, J. Zhou, T. Koschny, and C. M. Soukoulis, Science **306**, 1351 (2004).
[7] R. Shelby, D. Smith, and S. Schultz, Science **292**, 77 (2001).
[8] R. B. Greegor, C. G. Parazzoli, J. A. Nielsen, M. A. Thompson, M. H. Tanielian, and D. R. Smith, Appl. Phys. Lett. (to be published).
[9] C. G. Parazzoli, R. B. Greegor, J. A. Nielsen, M. A. Thompson, K. Li, A. M. Vetter, M. H. Tanielian, and D. C. Vier, Appl. Phys. Lett. **84**, 17 (2004).
[10] D. Schurig and D. R. Smith, Phys. Rev. E **70**, 065601 (2004).
[11] A. F. Starr, P. M. Rye, D. R. Smith, and S. Nemat-Nasser, Phys. Rev. B **70**, 113102 (2004).
[12] D. R. Smith, J. J. Mock, A. F. Starr, and D. Schurig, Phys. Rev. E **71**, 036609 (2005).